

Neuroprotective Role of Camel α -Lactalbumin Via Regulating SIRT1/FOXO3a Pathway Against Rotenone-Induced Neurotoxicity

Saba Ubaid

King George Medical University: King George's Medical University

Shivani Pandey (✉ dr.shivani111263@gmail.com)

King George Medical University: King George's Medical University <https://orcid.org/0000-0003-0421-5722>

Mohd. Sohail Akhtar

Central Drug Research Institute

Mohammad Rumman

King George's Medical University

Babita Singh

King George Medical University: King George's Medical University

Abbas Ali Mahdi

King George Medical University: King George's Medical University

Research Article

Keywords: Camel milk, α -Lactalbumin, oxidative stress, apoptosis, inflammation, SIRT1

Posted Date: July 8th, 2021

DOI: <https://doi.org/10.21203/rs.3.rs-595308/v1>

License:   This work is licensed under a Creative Commons Attribution 4.0 International License.

[Read Full License](#)

Abstract

Camel milk is rich in nutritional factors, such as α -Lactalbumin, and important for brain development. It is known to act as a potential therapeutic candidate for brain disorder via regulation of inflammatory and apoptotic pathways. Mechanisms that are critically involved with Parkinson's disease (PD) are apoptosis, inflammation, and oxidative stress, and the aberrated ubiquitin-proteasome system. Adverse effects of current therapies are imposing the need for the development of natural neuroprotective agents that are very effective and have fewer or no side effects. The present study aimed to evaluate the potential activity of camel α -Lactalbumin (α -LA) in rotenone induced in-vitro PD model. In this study, we hypothesized the use of camel α -lactalbumin as an effective curative agent for PD. The mechanism of action of camel α -lactalbumin was investigated by assessing the effect of α -LA on the level of nitric oxide, NADH, MMP9, inflammatory markers, and on the expression level of SIRT1 and FOXO3a in SH-SY5Y cell line. Overall, the results revealed the potent neuroprotective efficacy of α -Lactalbumin in rotenone-induced PD model via effectively modulating apoptotic pathways, oxidative stress, and neuroinflammatory cascades. Conclusively, these findings confirmed that α -LA could be a biologically effective protective agent against rotenone induced neurotoxic impacts and neurobehavioral aberrations.

Introduction

Recent researches reveal the traditional biological role of various milk proteins and peptides that can pose multiple functions and exerts various moon-lighting activities, such as immunomodulatory, antioxidant, and anti-inflammatory activity (Chen et al 2014). The attractiveness of using milk-derived biologics as a potential drug relies on the important fact that protein and peptides are well tolerated by organisms and exhibit oral bioavailability (Sakandar et al. 2018). Several pieces of evidence show the nutraceutical potential and health benefits of camel milk (Sakandar et al. 2018). Camel milk has high therapeutic potential against diabetes and cancer as well as possess anti-hypertensive and anti-oxidative properties (Sakandar et al. 2018). The major part of camel milk is α -Lactalbumin (α -LA) (Salami et al. 2009). The α -Lactalbumin protein is known for the synthesis of lactose in response to prolactin in the mammary gland (Kuhn et al.1980) and displays many biological properties. It has a globular structure composed of a large α -domain (regions 1–34 and 86–123) containing three α -helices and two 310 helices, and a small β -domain containing a three-stranded antiparallel β -sheet and a 310 helix and this globular structure is stabilized by four disulfide bonds and a calcium ion (Chandra et al. 1998; Chrysina et al. 2000). The binding of calcium confers resistance to enzyme proteolysis (Schmidt et al. 1991).

Camel α -Lactalbumin has several advantages such that it has high antioxidant power than bovine (Salami et al. 2009). It possesses a high nutritional interest as it contains a high concentration of essential amino acids (Swiss-Prot accession number P00710), higher than the bovine counterpart (Salami et al. 2009). Previous studies have been shown that supplementation with α -LA in adults enhanced the tryptophan and serotonin levels which are associated with improved cognition in stress vulnerable individuals.

In this study, we hypothesized the use of camel α -Lactalbumin as a therapeutic supplement for Parkinson's Disease. Parkinson's Disease (PD), is a prevalent neurodegenerative disorder among aging people. To date, the actual pathogenesis of degeneration of neurons in the substantia nigra pars compacta (SNc), remains obscure. Increasing evidence revealed that defects in the clearance of abnormal protein aggregates, generation of reactive oxygen species (ROS), inflammation, mitochondrial dysfunction, and endoplasmic reticulum stress to be the cardinal factors contributing to the pathogenesis of PD (Lin et al. 2006; Hashimoto et al. 2003; Gibson et al. 2004, Yacoubian et al. 2009).

A recent study also demonstrated that in response to oxidative stress, Silent information regulator (SIRT1) interacts with and deacetylates FOXO 3a, which increases its ubiquitination level and protected against apoptosis (wang et al. 2015).

Despite the several treatment strategies, complete treatment of PD is still not possible and the prolonged use of known treatments has several adverse effects. Considering the role of oxidative stress and inflammation as a major role in neurodegeneration, the focus is on investigating the agents of natural origin that has lesser or no side effect and have therapeutic potential and pharmacological properties to combat oxidative damage and neuroinflammation. In the present study, we evaluated the therapeutic potential of Camel α -lactalbumin in in-vitro studies of the rotenone-induced PD model.

Material And Method

Camel α -LA was purchased from Cusabio Biotech Co. Ltd, (Cat#CSB-YP012724 CYV Wuhan, China). Dulbecco's modified Eagle's medium/F12 (DMEM) were purchased from Gibco; Thermo Fisher Scientific, Inc (Waltham, MA, USA). Assay kits for cell viability (MTT Assay kit) was purchased from Abcam, ab211091 (Cambridge, MA 02139-1517 USA). HPLC standard of nicotinamide adenine dinucleotide (NADH). were purchased from Sigma-Aldrich Inc. (St. Louis, MO, USA). TRIzol was purchased from Sigma- Aldrich Inc. (St. Louis, MO, USA). Hi-Fi cDNA Synthesis Kit for conversion of RNA to cDNA was purchased from Abcam, ab185916, and the expression level of the gene was checked by Applied Biosystems™ PowerUp™ SYBR™ Green Master Mix. Nitric Oxide Assay Kit (Colorimetric) (ab65328) was purchased from Abcam (Cambridge, MA 02139-1517 USA). Human IL-8 and human MMP-9 ELISA kits were purchased from Raybiotech. Hoechst 33342 Staining Dye Solution 5ml, (ab228551), SIRT1 (ab189494), FOXO3a (ab109629), β -actin (ab8227) Goat Anti-Rabbit IgG H&L (HRP) (ab6721) antibodies were purchased from Abcam (Cambridge, MA 02139-1517 USA). ECL Western Blotting Substrate Kit (ab65623) was also purchased from Abcam (Cambridge, MA 02139-1517 USA).

2.1 Cell culture

SH-SY5Y neuroblastoma cell line was purchased from the National Center for Cell Science (NCCS), Pune, India. Cells were cultured in Dulbecco's Modified Eagle's Medium (DMEM) supplemented with 10% FBS and 1% antimycotic/antibiotic and maintained in a humidified incubator at 37° C with 5% CO₂ 95% air. Culture medium was replaced every after two days. Cells were pretreated with rotenone (500 nM) for 8 h and then incubated with α -LA (0.2 mg/ml) for 18 h.

2.2 Assessment of cell viability

Cell viability was assessed using the 1-(4,5-dimethylthiazol-2-yl)-3,5-diphenylformazan (MTT) assay kit. Briefly, the culture medium was discarded and 50 μ L serum free media with 50 μ L MTT solution was added into each well, and plates were incubated at 37 °C for 3 h. After incubation 150 μ L of MTT solvent was added into each well and the plate was wrapped with foil and kept for shaking on an orbital shaker for 15 min. Absorbance was recorded at 590 nm using 96 well microplate reader Synergy HT (Biotek).

2.3 Determination of NO accumulation in SH-SY5Y culture

Levels of NO were assessed using a NO assay kit. In brief, 2×10^6 cells were cultured in 96 well plate and after treatment, the cell culture media were washed with cold PBS. Cells were resuspended in 100 μ L of ice-cold Assay buffer, then homogenized and centrifuge for 2-5 min at 14000 rpm and 4°C temperature. Collected supernatant was transferred to a fresh tube and kept on ice. Nitrate reductase, enzyme cofactor, assay buffer, and samples were added into 96 well plate and incubated at room temperature for 1h to convert nitrate to nitrite. 1 μ L of enhancer were added into each well and incubated at room temperature for 10min. 50 μ L of Griess reagent R1 and 50 μ L of Griess reagent R2 were added and the intensity of the chromophore was used to determine the NO levels at 540 nm using 96 well microplate reader Synergy HT (Biotek).

2.4 Determination of NADH level

Cells were harvested, washed with PBS, and lysed by using 3% perchloric acid in methanol. The standard curve for NADH was generated by dissolving 1 mg of NADH in methanol (1 mg/ml). The concentration of NADH was measured by UV-HPLC (Agilent) using a C18 column (Eclipse plus C18, particle size 5 μ m column size (4.6 \times 25 mm)). The mobile phase was composed of Solvent A: 0.2 M sodium acetate pH 4.8 and Solvent B: methanol. The time program used was: Solvent A: 90% (v/v), Solvent B: 10% (v/v) flow rate was 1 ml/min. The analysis was completed within 11 min. UV detection was performed at 220, 260, and 280 nm. Data was acquired using CP Open Lab Control Panel.

2.5 Dual Staining

Acridine orange and ethidium bromide fluorescent probes were used to analyze apoptosis by fluorescent microscopy. After the treatment schedule as described in the previous experiment, the medium was removed from the plating cell (1×10^5) were washed with PBS twice stained with 100 μ g/ml of AO/EB stain. To remove excess dye cells were incubated for about 20 min at room temp and then washed with warm PBS. Fluorescent microscopy was used for morphological studies and photography.

2.6 Hoechst nuclear Staining

After the treatment cells were washed with PBS and incubated with Hoechst 100ng/ml in PBS in the dark for 15 min. at room temperature. Cells were again washed with PBS after Hoechst staining in PBS for 5 min at room temperature and visualized by using the fluorescence microscope.

2.7 Determination of the level of IL-8 and MMP-9

Level of IL-8 and MMP-9 were determined through the ELISA kit according to the manufacturer's protocol.

2.8 Molecular Docking

Protein Data Base ID of SIRT1 (ID:4I5I) & PubChem ID of rotenone (ID:6758) was used in cDock software for protein-ligand interaction. For the docking of SIRT1 and camel α -LA uniport was used for the FASTA format and docking pattern was recorded in HDock. Hydrogen atoms and charges were added while all the crystallographic water molecules were removed.

2.9 Measurement of gene expression

Total RNA was isolated from the cells by using TriZol and its quality was checked by agarose gel electrophoresis. RNA was converted to cDNA using a cDNA synthesis kit according to the manufacturer's protocol. Quantitative real-time PCR (qPCR) was performed using Syber green master mix in triplicate using Applied Biosystems 7500 fast real-time PCR System.

Relative gene expression was determined by a comparative threshold cycle and normalized against β actin. Ct value of the genes was normalized using the formula $\delta Ct = Ct_{\text{gene}} - Ct_{\beta \text{ actin}}$. The primer sequence used is as follows;

Beta actin

FP-TCCACGAACTACCTTCAACTC

RP- CAGTGATCTCCTTCTGCATCC

SIRT1

FP- AGAACCCATGGAGGATGAAAG

RP TCATCTCCATCAGTCCCAAATC

FOXO3a

FP- AGAGCTGAGACCAGGGTAAA

RP-GACAGGCTTCACTACCAGATTC

2.10 Measurement of Protein expression level

Total protein was isolated by using the ice cold RIPA buffer supplemented with protease inhibitor and cell debris was removed by centrifugation at 1400 rpm for 20 min. protein concentration was evaluated by BCA kit and then the protein sample (30 μ g) was separated by 12 % SDS polyacrylamide gel

electrophoresis and transfer to the PVDF membrane. After protein transfer, the membrane was blocked with 5 % skimmed milk in PBST and shake on a shaker for 1 hour at room temperature. The membrane was washed 3 times with PBS and probed with rabbit monoclonal 1⁰ antibodies against SIRT1, FOXO3a, and with rabbit polyclonal antibody against β -actin followed by incubation with horseradish peroxidase conjugated Goat Anti Rabbit IgG H&L 2⁰ antibody.

Immunoblots were developed with ECL western blotting substrate kit. The bands were scanned and quantified by densitometer analysis after normalization with β -actin.

2.11 Statistical Analyses

Data are expressed as mean \pm SEM. Statistical analyses were performed through one-way ANOVA followed Bonferroni multiple comparisons test by using GraphPad Prism 5.0 software. A probability value of less than 0.05 was considered to be statistically significant.

Result

3.1 Effect of α -LA against rotenone-induced neurotoxicity in SHSY-5Y cells.

α -LA was screened for its ability to protect human neuronal SH-SY5Y cells against oxidative damage using MTT assay. Briefly, SH-SY5Y cells were treated with varying concentrations (1 mg/ml, 0.5 mg/ml, 0.2 mg/ml) of α -LA for 24 h. Results showed very little toxicity effects at 1 and 0.5 mg/ml of α -LA while 0.2 mg/ml showed no toxicity (Fig. 1b). Then the effect of α -LA on rotenone-treated (500 nM) neuronal cells was determined. Results showed significantly high cell viability in α -LA treated cells as compared to rotenone treated cells (Fig. 1c). Additionally, the neuroprotective effect of α -LA was also confirmed by morphological observation (Fig. 1a). Morphological changes were observed in 500 nM rotenone-treated cells, showing retracted neurites with small round structures while α -LA treatment prevented the abnormal morphological changes in the cells.

3.2 α -LA reduced rotenone-induced apoptosis

To characterize the apoptotic profiles, SH-SY5Y cells were stained with AO/EB after rotenone- and α -LA treatment. Dual staining was examined under a fluorescence microscope. Healthy cells are marked by granular yellow-green color AO nuclear staining while EB penetrates only on the apoptotic cells and shows red color. As the results showed that in rotenone-treated culture, more cells seem to be red which reveals that cells undergo apoptosis upon rotenone treatment, while in α -LA treated culture, only a few cells were red as compared to rotenone treated cells. The Hoechst nuclear staining clearly shows apoptosis following rotenone treatment and supports the data on the protective effect of α -LA against DNA fragmentation.

3.3 α -LA reduces cellular production of NO

Nitric oxide production was found to significantly increase in rotenone-treated cells, while it was lower in α -LA treated cells (Fig. 3)

3.4 α -LA mitigates inflammatory cytokines expression.

Tumor necrosis factor α (TNF α), IL-1 β , IL-8 are important mediators that activate and propagate neuroinflammation. We, therefore, determined the level of these inflammatory cytokines in SH-SY5Y cells. Rotenone treatment induced a rise in the level of TNF α , IL-1 β , and IL-8 as compared to control. Interestingly, α -LA-treatment to rotenone-treated cells significantly decreases ($p < 0.05$) the level of inflammatory cytokines when compared to rotenone- treated cells (Fig. 4).

3.5 α -LA enhances NADH levels

To elucidate the potential molecule mechanism of α -LA against rotenone-induced neurodegeneration, we measured the level of NADH using HPLC (Fig. 5). NADH ubiquinone oxidoreductase activity is inhibited by the binding of rotenone to ubiquinone. HPLC analysis reveals that the NADH level was high in rotenone exposed cells and its level significantly reduced in the α -LA treated group as compared to rotenone treatment.

3.6 α -LA exerts neuroprotection by inhibiting matrix metalloproteinase expression

MMP-9 plays an important role as an initiator of neuro-inflammation. Here, we assessed if α -LA could alleviate MMP-9 expression that may diminish pro-inflammatory response upon rotenone challenge. As shown in Fig. 6 rotenone administration significantly ($p < 0.05$) elevated the expression of MMP-9 as compared to control. Interestingly α -LA treatment suppressed MMP-9 mediated inflammation by dampening the MMP-9 activity.

3.7 α -LA could bind to SIRT1 and up-regulate the expression of SIRT1 in rotenone Induced SH-SY5Y cells

Docking software was used to evaluate whether SIRT1 can interact with α -LA where rotenone binds and forecast their docking pattern and docking score. Result of molecular docking revealed that the docking score of α -LA to SIRT1 was -237.23 with Tm score 0.9925, which forms a stable docking pattern (Fig. 6c). α -LA molecules falls inside the active pocket of protein Sirt1 (Fig. 6c). The calculation forecasted that α -LA molecules could directly interact to protein SIRT1 and their interphase of interaction shows in the supplementary data. The result above indicated that α -LA and SIRT1 have affinity, and α -LA was likely to regulate the pharmacological effect of SIRT1. We found that the protective effect of α -LA on rotenone induced PD model was due to its binding to SIRT1 and their vina score shows in supplementary table. Followed by the RT-PCR result, SIRT1 and FOXO3a (the downstream protein of SIRT1) protein expression were significantly downregulated after rotenone exposure on SH-SY5 cells, and α -LA reversed this phenomenon.

3.8 Effect of α -LA on activation of SIRT1-FOXO3a signaling pathway

To better understand the molecular mechanism involved in the neuroprotective activity of α -LA, we determined the expression level of SIRT1 and FOXO 3a in rotenone-induced Parkinson's cell model. As expected rotenone-treated cells had significantly reduced expression of SIRT1 and FOXO3a as compared to the control group, while their expression was relatively high in α -LA treated cells as compared to rotenone treated cells as determined through RT-PCR (Fig. 7) and western blot (Fig. 8).

Discussion

Interest in the use of camel milk for human nutrition has increased during the last decade as evidenced by several review articles reporting the nutraceutical potential and health benefits of this milk. For instance, camel milk possesses efficient therapeutic properties against diabetes and cancer and for anti-hypertension (Sakandar et al. 2018). Camel milk contains an important protein, known as α -lactalbumin, which is a small calcium-binding globular protein. Historically α -LA is best known for its ability to bind calcium ions and regulate the synthesis of lactose. It constitutes up to 20 % of total milk protein and is now known to have a multitude of biological activities (Permyakov et al. 2016; Permyakov et al. 2016; Uversky et al. 2016). A majority of research was conducted using human and bovine α -lactalbumin, whereas little is known about the camel α -LA. Camel milk and related product are important nutritional sources in various regions of the world. In this study, we showed that α -lactalbumin has a neuroprotective effect on the rotenone-induced PD cell model through anti-oxidative, anti-apoptotic, and anti-inflammatory effects. Thus, it could be expected that α -LA can provide new potential for the treatment of PD.

NADH plays a critical role in energy metabolism and also in cell death and various cellular function including, gene expression and regulation of calcium homeostasis. It has been indicated that NADH is a mediator of various major biological processes including aging and regulates numerous enzymes including dehydrogenase, Sirtuins, poly (ADP-ribose) polymerase, mono (ADP-ribosyl) transferase, and ADP ribosyl cyclase. (Ying W., et al 2006). NADH was reported to be reduced in PD. NADH is also known to stimulate tyrosine hydroxylase and dopamine biosynthesis. Administration of NADH in PD treatment improves the patient's condition. Our result shows that α -LA treatment is sufficient in enhancing the level of NADH from this we can conclude that it can enhance dopamine in PD patients.

Previous literature showed that MMP9 plays an important role in neurogenesis, myogenesis, axonal guidance as well as supporting synaptic plasticity, learning, and memory (Yong et al 2005 and Agrawal 2008). MMP9 is known to mediate inflammation-mediated neuroinflammation. Besides, MMPs are also influenced by oxidative stress (Choi et al., 2008). MMP9 is present in the tertiary granule of neutrophils and can be released on stimulation. The increasing level of IL8, IL-1, and TNF- α contribute to elevating MMP-9 concentration (Weddt et al., 2004 and Sudeep Chakraborty). Overexpression of MMP9 and its release at synapse may destroy the structural integrity of the surrounding ECM (Lim et al 1996). It is also known that alpha-synuclein in rat primary astrocytes increases MMP9 activity by stimulating microglial to activate microglia PAR-1 and amplify microglial inflammation signal (Lee et al 2010 and Joo SH et al 2010). Treatment with MMP 9 inhibitor attenuated the neuronal cell death induced by 6OHDA and

MPP(+)(Joo SH). As shown in our result α -LA decreases the MMP-9, IL- β , TNF- α , and IL-8 in the rotenone-induced PD model that in turn reduces the neuroinflammation.

SIRT1 is a well-known cell survival protein related to neuroprotection, localized mainly in the nucleus. In this study, we demonstrated that the neuroprotective effects of α -LA on rotenone induced oxidative damage might be related to the suppression of ROS generation, activation of SIRT1-FOXO3a, and enhancement of antioxidant enzymes. We adopted docking to evaluate whether SIRT1 could bind to α -LA and the result showed that α -LA could bind to SIRT1. α -LA likely upregulated protein expression of SIRT1 as well as FOXO3a under oxidative stress. Importantly, SIRT1 protein act as an upstream regulator on several transcription factors, for instance, FOXO3a which controls ROS generation, apoptosis, and mitochondrial dynamics (Canto et al. 2009; Haigis et al. 2010; Ng et al. 2015; Gay et al. 2018; Gay et al. 2018). FOXO3a declines and its expression appears to be disturbed in all age-dependent neurodegenerative diseases (Kim et al. 2014). FOXO3a is involved in the detoxification of ROS by upregulating endogenous antioxidant enzymes including SOD2 and CAT30, and modulation of DNA repair and cell apoptosis. As the morphological analysis of Hoechst and dual staining showed that α -LA prevent the apoptosis that was induced by rotenone. Significant upregulation of SIRT1 and FOXO3a by α -LA is observed in rotenone-induced neuronal cells, thereby suggesting their roles in neuroprotection as the SIRT1-FOXO3a axis is a conserved cell survival pathway that mitigates oxidative stress insults and apoptosis.

Conclusion

α -LA has pleiotropic actions and it acts through multiple channels. This study shows that α -LA improves the pathological changes in the PD model by activating SIRT1, which led to FOXO3a upregulation and prevents oxidative stress and apoptosis. α -LA enhances the level of NADH that may improve the level of dopamine in PD for this further research needs to prove that it enhances the level of dopamine. α -LA downregulates the expression of IL-1 β , and TNF- α and lowers the level of IL-8 and MMP-9 from this we can conclude that it can reduce inflammation. However, to better elucidate α -LA mechanisms of action further in vivo and clinical studies are still needed.

Abbreviations

PD, Parkinson's disease; α -LA, Camel α -lactalbumin; HPLC, high performance liquid chromatography; NADH, nicotinamide adenine dinucleotide; SIRT1, Silent Information Regulator 1; FOXO3a, Forkhead box O, NO, Nitric oxide.

Declarations

Authors contributions

S.U. designed, performed, and interpreted the experimental analyses and manuscript preparation. S.P. was responsible for the accuracy of any part of the work. M.S.A. performed the analysis of protein expression. M.R. and B.S. revised the manuscript and A.A.M. provides resources. All authors read and approved the manuscript and all data were generated in-house and that no paper mill was used.

Acknowledgements

This study was supported by the Ministry of Science & Technology Department of Biotechnology (No. BT/IN/Indo-US/Foldscope/39/2015) and Indian Council of Medical Research (3/1/2/76/Neuro/2018-NCD-I).

Data availability

Original source data and all immunoblots are presented completely as supplementary material.

Ethics declarations

Conflict of interest

The authors declare that they have no conflict of interest.

Ethical approval

Not applicable.

References

1. Chen YF, Mollstedt H, Tsai O, Kreider MH RB (2014) Potential clinical applications of multi-functional milk proteins and peptides in cancer management. *Curr. Med. Chem* Jul 1;21(21):2424-37
2. Sakandar HA, Ahmad S, Perveen R, Aslam HK, Shakeel A, Sadiq FA, Imran M (2018) Camel milk and its allied health claims: a review. *Prog. Nutr* Jul 1;20(Supplement 1):15–29
3. Salami M, Yousefi R, Ehsani MR, Razavi SH, Chobert JM, Haertlé T, Saboury AA, Atri MS, Niasari-Naslaji A, Ahmad F, Moosavi-Movahedi AA (2009) Enzymatic digestion and antioxidant activity of the native and molten globule states of camel α -lactalbumin: Possible significance for use in infant formula. *Int Dairy J* Sep 1;19(9):518 – 23
4. Kuhn NJ, Carrick DT, Wilde CJ (1980) Lactose synthesis: the possibilities of regulation. *J dairy Sci* Feb 1;63(2):328 – 36
5. Chandra N, Brew K, Acharya KR (1998) Structural evidence for the presence of a secondary calcium binding site in human α -lactalbumin. *Biochemistry* Apr 7;37(14):4767-72
6. Chrysina ED, Brew K, Acharya KR (2000) Crystal structures of apo-and holo-bovine α -lactalbumin at 2.2-Å resolution reveal an effect of calcium on inter-lobe interactions. *J Biol Chem* Nov 24(47):37021–37029 275(

7. Schmidt DG, Poll JK (1991) Enzymatic hydrolysis of whey proteins. Hydrolysis of α -lactalbumin and β -lactoglobulin in buffer solutions by proteolytic enzymes. *Nederlands melk en Zuiveltijdschrift* 45(4):225–240
8. Lin MT, Beal MF (2006) Mitochondrial dysfunction and oxidative stress in neurodegenerative diseases. *Nature* Oct 443(7113):787–795
9. Hashimoto M, Rockenstein E, Crews L, Masliah E (2003) Role of protein aggregation in mitochondrial dysfunction and neurodegeneration in Alzheimer's and Parkinson's diseases. *Neuromolecular Med* Oct 4(1):21–35
10. Gibson GE, Huang HM (2004) Mitochondrial enzymes and endoplasmic reticulum calcium stores as targets of oxidative stress in neurodegenerative diseases. *J Bioenerg Biomembr* Aug 36(4):335–340
11. Yacoubian TA, Standaert DG (2009) Targets for neuroprotection in Parkinson's disease. *Biochim Biophys Acta Mol Basis Dis* Jul 1;1792(7):676 – 87
12. Wang YQ, Cao Q, Wang F, Huang LY, Sang TT, Liu F, Chen SY (2015) SIRT1 protects against oxidative stress-induced endothelial progenitor cells apoptosis by inhibiting FOXO3a via FOXO3a ubiquitination and degradation. *J Cell Physiol* Sep 230(9):2098–2107
13. Permyakov A, Permyakov EE, Breydo S, Redwan LM, Almehdar E, Uversky HN V (2016) Disorder in milk proteins: α -Lactalbumin. Part C. Peculiarities of metal binding. *Curr Protein Pept Sci* Dec 1;17(8):735 – 45
14. Permyakov EA, Permyakov SE, Breydo L, Redwan EM, Almehdar HA, Uversky VN (2016) Disorder in milk proteins: α -lactalbumin. Part A. Structural properties and conformational behavior. *Curr Protein Pept Sci* 17:352–367
15. Uversky N, Permyakov VE, Breydo S, Redwan LM, Almehdar E, Permyakov HA E (2016) Disorder in milk proteins: α -Lactalbumin. Part B. A multifunctional whey protein acting as an oligomeric molten globular “oil container” in the anti-tumorigenic drugs, lipotides. *Curr Protein Pept Sci* Sep 1;17(6):612 – 28
16. Ying W (2006) NAD⁺ and NADH in cellular functions and cell death. *Front Biosci* Sep 1;11(1):3129-48
17. Yong VW (2005) Metalloproteinases: mediators of pathology and regeneration in the CNS. *Nat Rev Neurosci* Dec 6(12):931–944
18. Agrawal SM, Lau L, Yong VW (2008) MMPs in the central nervous system: where the good guys go bad. *Semin Cell Dev Biol* Feb 1 (Vol. 19, No. 1, pp. 42–51). Academic Press
19. Choi DH, Kim EM, Son HJ, Joh TH, Kim YS, Kim D, Flint Beal M, Hwang O (2008) A novel intracellular role of matrix metalloproteinase-3 during apoptosis of dopaminergic cells. *J Neurochem* Jul 106(1):405–415
20. Weydt P, Yuen EC, Ransom BR, Möller T (2004) Increased cytotoxic potential of microglia from ALS-transgenic mice. *Glia*. Nov 1;48(2):179 – 82
21. Chakrabarti S, Patel KD (2005) Regulation of matrix metalloproteinase-9 release from IL-8-stimulated human neutrophils. *J Leukoc Biol* Jul 78(1):279–288

22. Lim GP, Backstrom JR, Cullen MJ, Miller CA, Atkinson RD, Tökés ZA (1996) Matrix metalloproteinases in the neocortex and spinal cord of amyotrophic lateral sclerosis patients. *J Neurochem* Jul 67(1):251–259
23. Andrew J, Lees JH, Tamas Revesz (2009) Parkinson's disease. *Lancet* 373:2055–2066
24. Joo SH, Kwon KJ, Kim JW, Kim JW, Hasan MR, Lee HJ, Han SH, Shin CY (2010) Regulation of matrix metalloproteinase-9 and tissue plasminogen activator activity by alpha-synuclein in rat primary glial cells. *Neurosci Lett* 29(3):352–356 469(
25. Cantó C, Gerhart-Hines Z, Feige JN, Lagouge M, Noriega L, Milne JC, Elliott PJ, Puigserver P, Auwerx J (2009) AMPK regulates energy expenditure by modulating NAD + metabolism and SIRT1 activity. *Nature* 458(7241):1056–1060
26. Haigis MC, Yankner BA (2010) The aging stress response. *Mol cell* 22;40(2):333 – 44
27. Ng F, Wijaya L, Tang BL (2015) SIRT1 in the brain—connections with aging-associated disorders and lifespan. *Front cell Neurosci* 9:9:64
28. Gay NH, Phopin K, Suwanjang W, Ruankham W, Wongchitrat P, Prachayasittikul S, Prachayasittikul V (2018) Attenuation of oxidative stress-induced neuronal cell death by *Hydnophytum formicarum* Jack. *Asian Pac J Trop* 11(7)(1):415
29. Gay NH, Phopin K, Suwanjang W, Songtawee N, Ruankham W, Wongchitrat P, Prachayasittikul S, Prachayasittikul V (2018) Neuroprotective effects of phenolic and carboxylic acids on oxidative stress-induced toxicity in human neuroblastoma SH-SY5Y cells. *NeurochemiRes* 43(3):619–636
30. Kim AD, Kang KA, Piao MJ, Kim KC, Zheng J, Yao CW, Cha JW, Hyun CL, Kang HK, Lee NH, Hyun JW (2014) Cytoprotective effect of Eckol against oxidative stress-induced mitochondrial dysfunction: Involvement of the Foxo3a/Ampk pathway. *J cell Biochem* 115(8):1403–1411

Figures

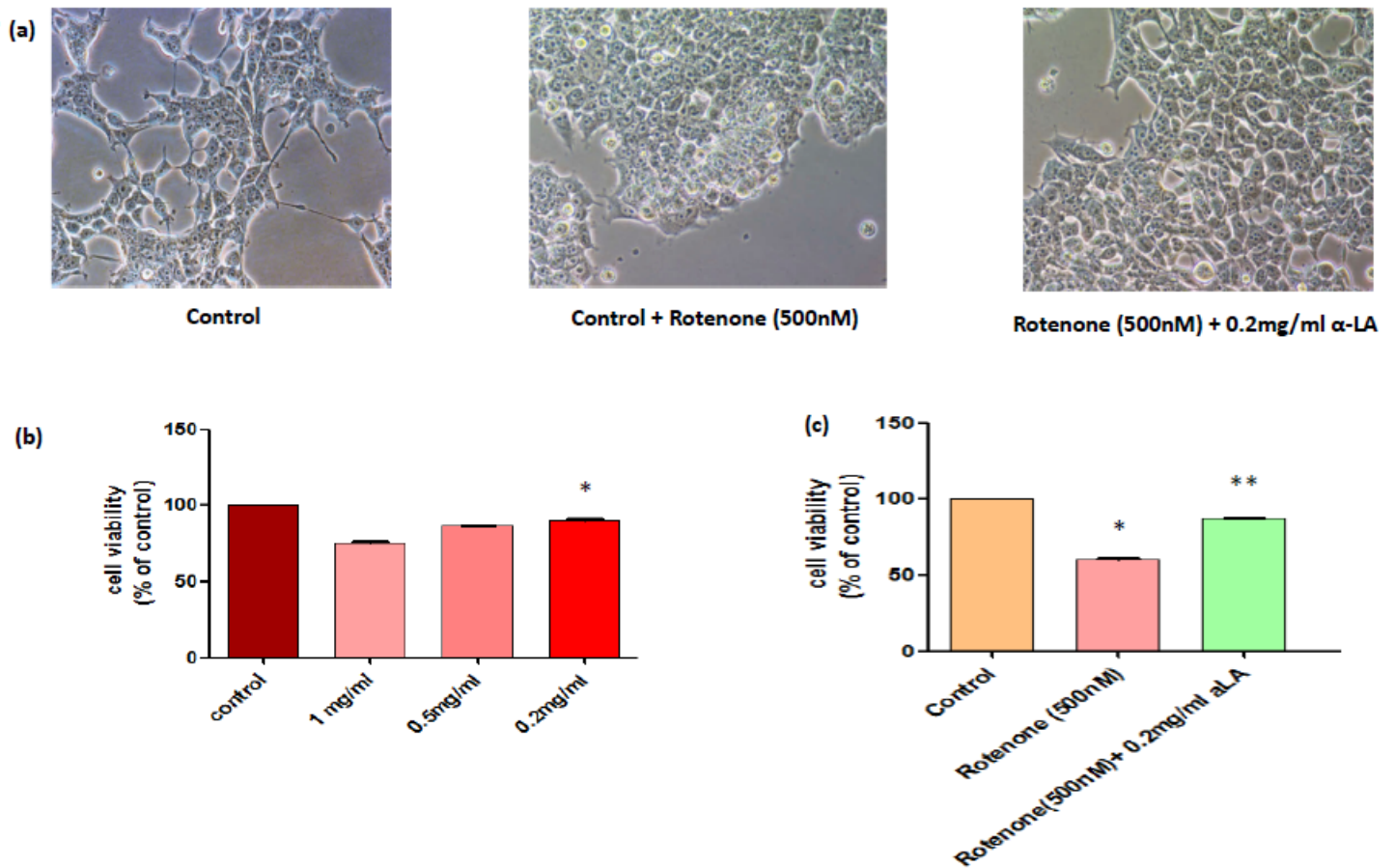


Figure 1

Effect of α-LA in rotenone-induced Parkinson's model (a) Morphological observation of SHSY-5Y cell line. (b) Shows the dose dependent effect of α-LA (1 mg/ml, 0.5 mg/ml, 0.2 mg/ml) (c) MTT assay to assess the cell viability in control, control + rotenone (500nM), rotenone (500nM) + α-LA (0.2 mg/ml). Data represent the mean ± S.E.M., n=6 (duplicates from 3 individual experiments) *P<0.05 as compared to control, **P<0.05 as compared to rotenone treated group.

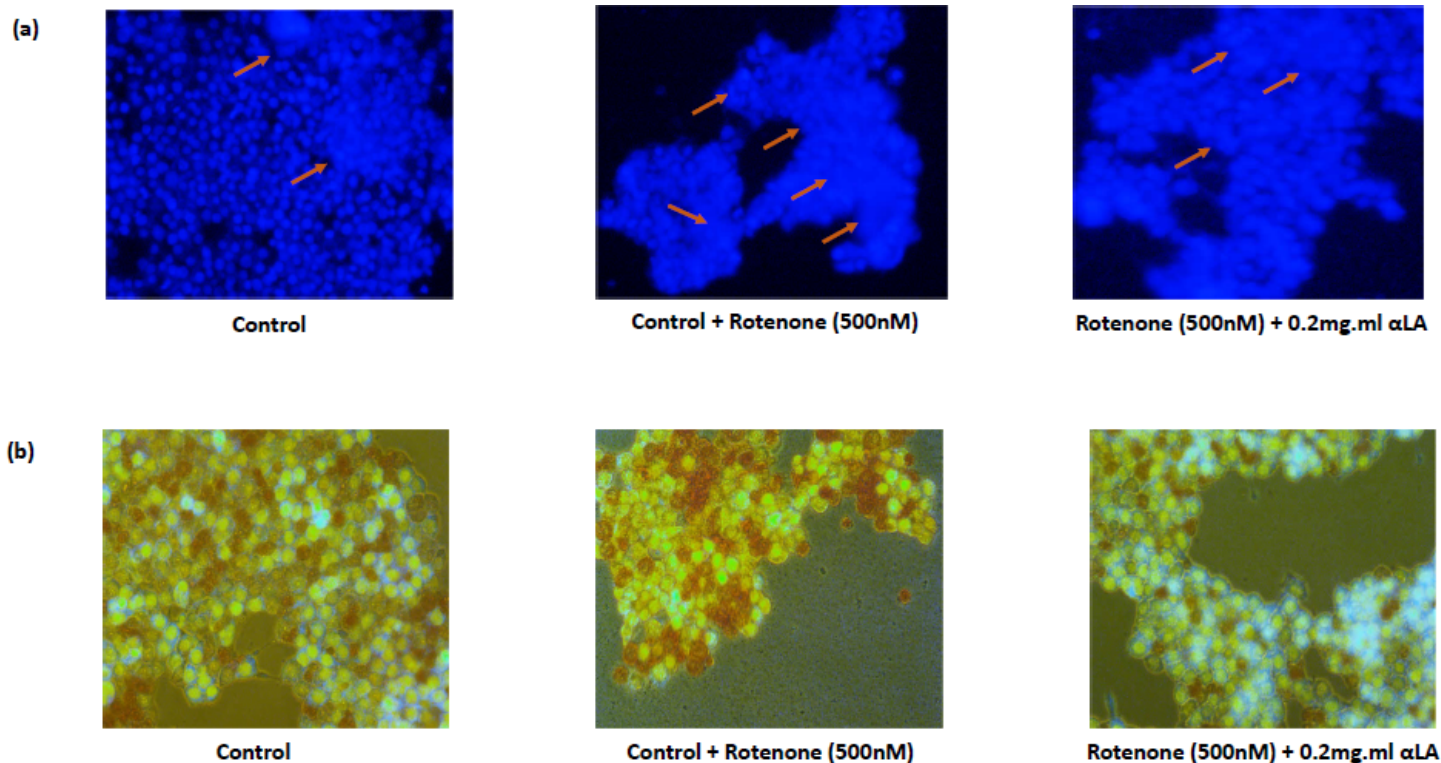


Figure 2

Protective effect of α -LA against rotenone-induced apoptosis (a) Hoechst nuclear staining was used to identify the live cells. Visual representation of typical apoptotic cells characterized by phase-bright nuclear fragmentation with rotenone treatment (red arrows were represented as apoptotic cells). (b) Dual staining was used to identify the live and apoptotic cells. Normal cells showed yellow-green fluorescence by acridine orange and dead cells showed uneven orange-red fluorescence by ethidium bromide.

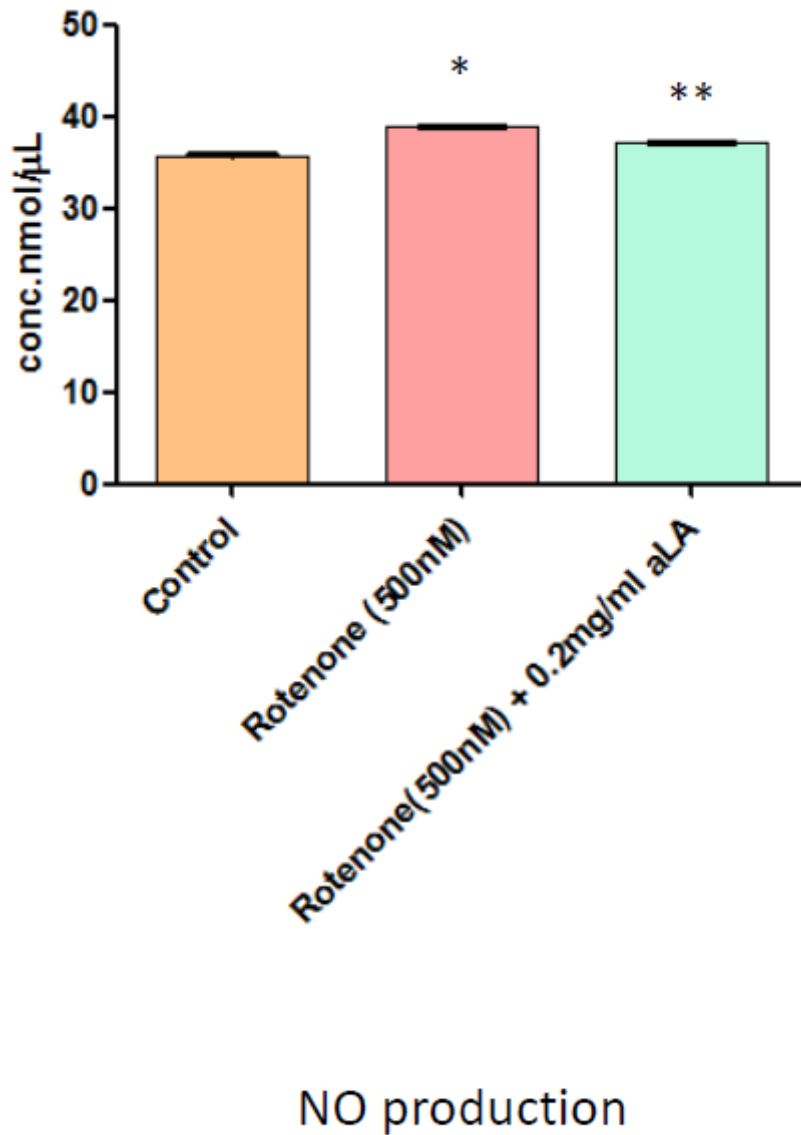


Figure 3

α-LA treatment prevented nitric oxide production and reversed antioxidant loss. Data represent the mean ± S.E.M., n=6 (duplicates from 3 individual experiments) *P<0.05 as compared to control., **P<0.05 as compared to rotenone treated group.

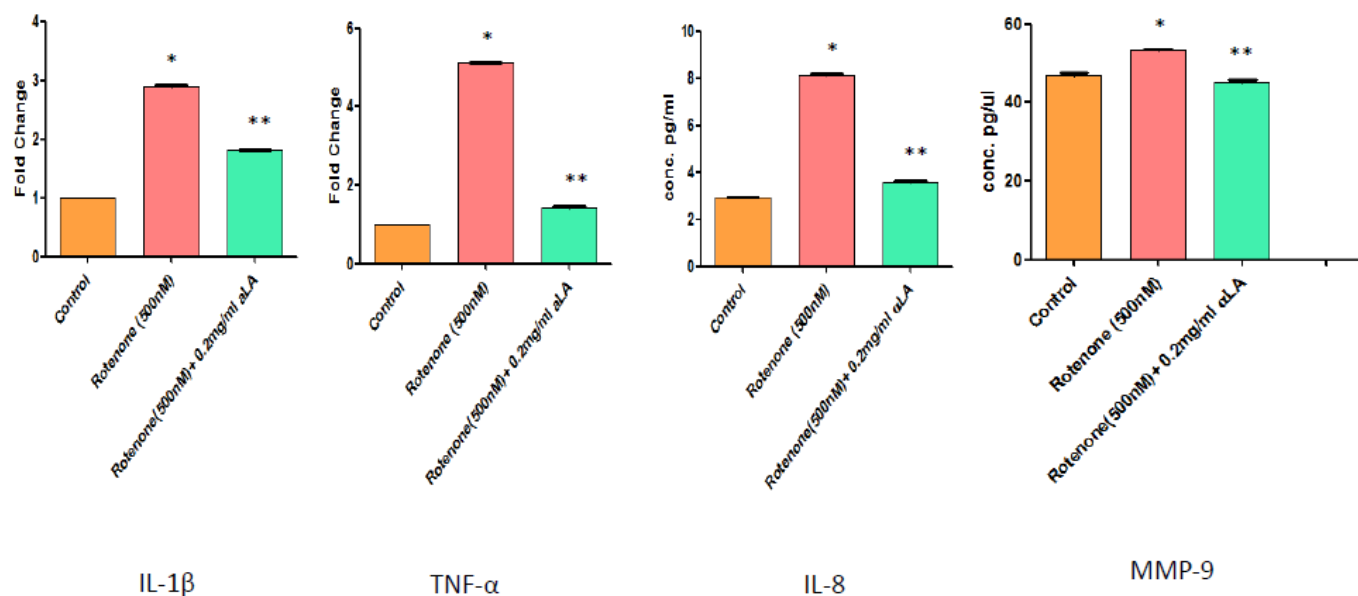


Figure 4

RT-PCR analysis showed that the rotenone administration increased the expression of IL-1 β , TNF- α . However, α -LA treatment significantly decreased the expression of IL-1 β , TNF- α in rotenone treated cell line. Enzyme linked Immunosorbent assay showed that rotenone administration increased the expression IL-8 and MMP-9 while the α -LA treatment significantly decreased the expression IL-8 and MMP-9. Data represent the mean \pm S.E.M., n=6 (duplicates from 3 individual experiments) *P<0.05 as compared to control, **P<0.05 as compared to rotenone treated group.

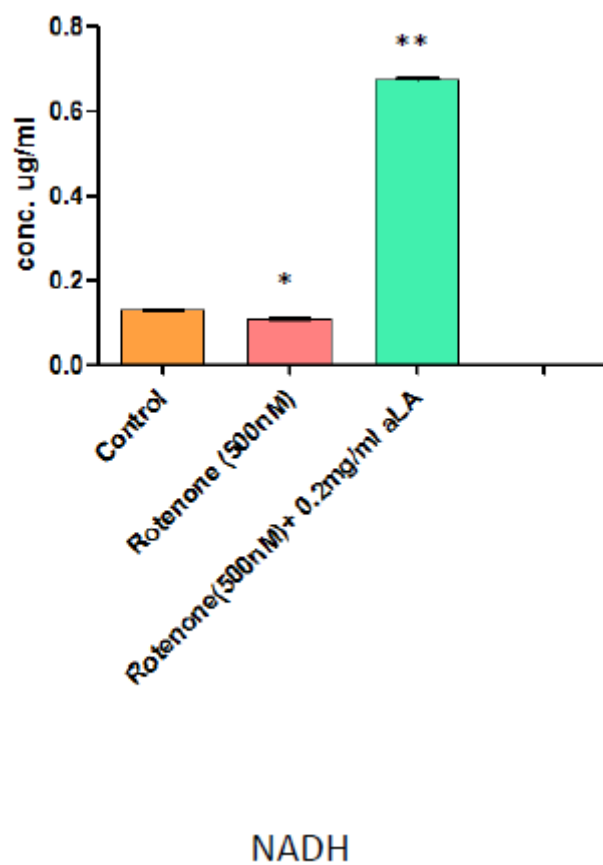


Figure 5

High Performance Liquid chromatography of NADH in control, control + rotenone (500nM), rotenone (500nM) + α -LA (0.2 mg.ml). Data represent the mean \pm S.E.M., n=6 (duplicates from 3 individual experiments) *P<0.05 as compared to control., **P<0.05 as compared to rotenone treated group.

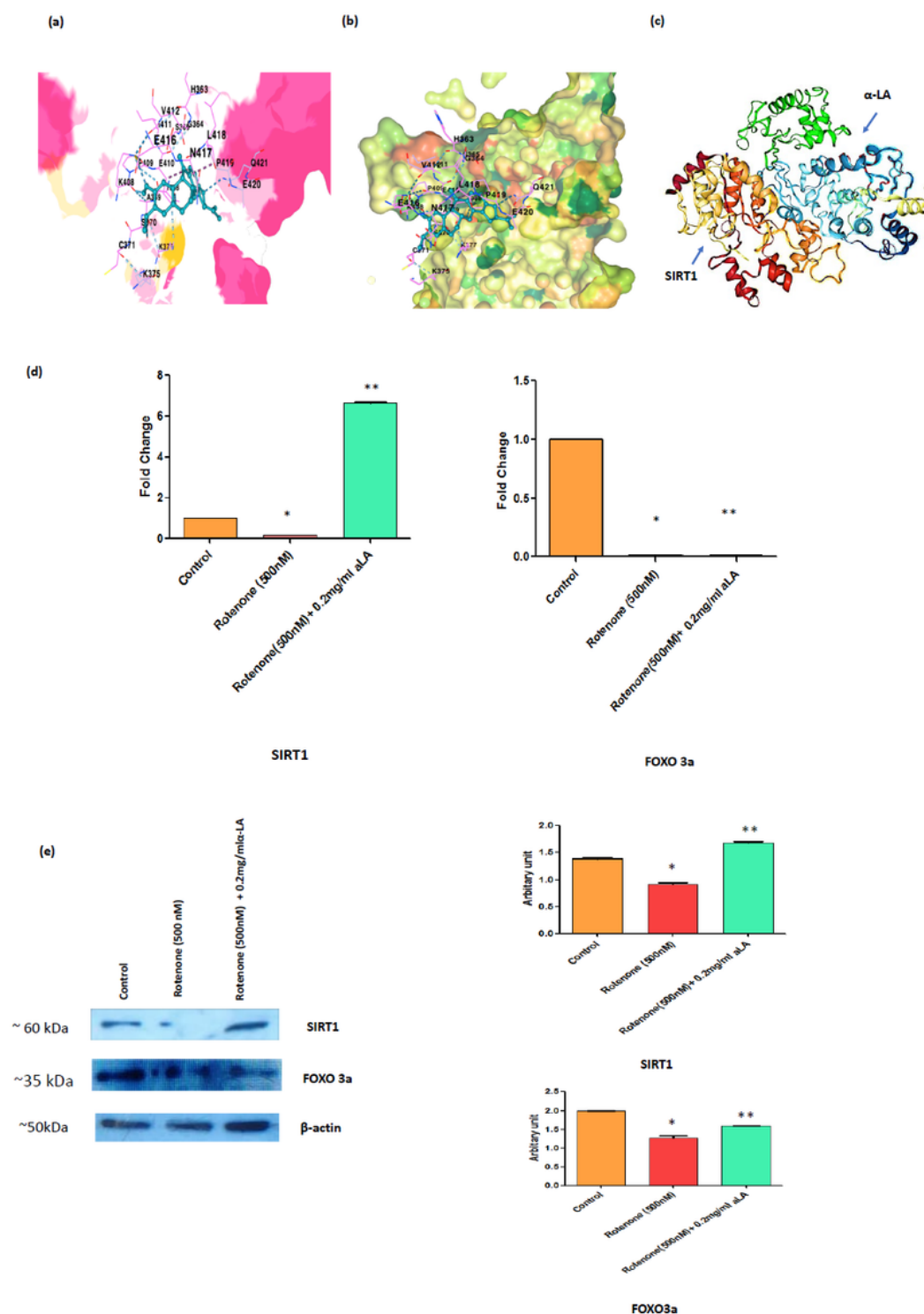


Figure 6

α-LA binds to SIRT1 and upregulates the expression of SIRT1 and FOXO3a in rotenone-induced SH-SY5Y cells. (a) The docked complex structure of SIRT1 and rotenone. Rotenone is shown in turquoise colour and the dashed line represents the hydrogen bonds between SIRT1 and rotenone. The number represents the amino acids of the SIRT1 protein that interact with rotenone. (b) SIRT1 protein surface and rotenone docked model. (c) Docking pattern of the ribbon-shaped structure of the catalytic domain of SIRT1 and α-

LA. (d) Bar diagram showing expression of SIRT1 and FOXO 3a at mRNA levels in control, control + rotenone (500nM), rotenone (500nM) + α -LA (0.2 mg.ml). Data represent the mean \pm S.E.M., n=6 (duplicates from 3 individual experiments) *P<0.05 as compared to control, **P<0.05 as compared to rotenone treated group. (e) Western blot analysis of SIRT1 and FOXO3a. The densitometric analysis was performed by normalizing SIRT1 and FOXO3a to those of β -actin in control, control + rotenone (500nM), rotenone (500nM) + α -LA (0.2 mg.ml). Data represent the mean \pm S.E.M., n=6 (duplicates from 3 individual experiments) *P<0.05 as compared to control, **P<0.05 as compared to rotenone treated group.

Supplementary Files

This is a list of supplementary files associated with this preprint. Click to download.

- [Graphicalabstract.png](#)
- [supplementary.pdf](#)